WHY IS (111) SILICON A BETTER MECHANICAL MATERIAL FOR MEMS ?

Jongpal Kim, Dong-il (Dan) Cho*, Richard S. Muller**

School of Electrical Engineering and Computer Engineering, Seoul National University, San 56-1, Shinlim-dong, Kwanak-gu, Seoul 151-742, Korea, *dicho@asri.snu.ac.kr

**Department of Electrical Engineering and Computer Sciences, University of California at Berkeley, Berkeley, CA 94720-1774, USA

SUMMARY

In this paper, we explain the mechanical properties of single-crystalline silicon with respect to deflectional and torsional motions. Young's modulus, Poisson's ratio, and shear modulus are isotropic on silicon (111), whereas the variations on silicon (100) and (110) are quite significant. We newly derive formulae for bulk shear modulus of silicon (100), (110) and (111) and show that bulk shear modulus differs from conventional shear modulus because of the anisotropic characteristics of single-crystal silicon. Furthermore, we show that the bulk shear modulus (which governs torsional motion) varies minimally on silicon (111), with respect to crystallographic directions, as compared to silicon (100) and (110).

Keywords: (111) silicon, Young's modulus, Poisson's ratio, shear modulus, torsional stiffness, bulk shear modulus

INTRODUCTION

Recently, many High Aspect Ratio Structures (HARS) micromachining technologies have been developed using single-crystal silicon, examples include, Single Crystal Reactive Etching And Metalization (SCREAM), Silicon On Insulator (SOI), Dissolved Wafer Process (DWP), Porous Si Method (PSM), and the Surface/Bulk Micromachining (SBM) processes [1-11]. These single-crystalline silicon structures have different mechanical charactersitics with respect to crystalline orientation because single-crystalline silicon is an anisotropic material. Young's modulus, Poisson's ratio, shear modulus, and bulk shear modulus are material constants that describe mechanical characteristics, and may have different values with respect to crystallographic orientation. Therefore, to properly design devices composed of such silicon based anisotropic materials and for which such mechanical properties are important, the mechanical properties of silicon (100), (110), and (111) were investigated.

YOUNG'S MODULUS, POISSON'S RATIO, AND SHEAR MODULUS

It is well known that Young's modulus, Poisson's ratio, and shear modulus are transversely and vertically isotropic for silicon (111), whereas these vary significantly for silicon (100) and (110) [12, 13].
Young's modulus, Poisson's ratio, and shear modulus can be derived from the general Hooke's law, in which 6 stress components are related to 6 strains by a stiffness matrix containing 3 independent components [14, 15]. As shown in Fig. 1, for silicon (100) and (110), Young's modulus varies from 130.2 GPa to 187.5 GPa, Poisson's ratio varies from 0.064 to 0.361, and shear modulus varies from 50.92 GPa to 79.4 GPa. For silicon (111), Young's modulus is transversely isotropic at 168.9 Gpa, regardless of the crystallographic orientation. Poisson's ratio has a constant value of $\nu_{//} = 0.262$ for planes parallel to (111), and a constant value of $\nu_{\perp} = 0.182$ for planes vertical to (111). Shear modulus is also a constant at $G_{//} = 66.9$ GPa for planes parallel to (111), and $G_{\perp} = 57.8$ GPa for planes vertical to (111).

TORSIONAL STIFFNESS AND BULK SHEAR MODULUS

Recent interests in optical applications of MEMS have resulted in many micromirrors supported by torsion springs [17]. In torsion beams, the resultant couple of the shear stresses acting over the cross section must be statically equivalent to the internal torque. Using this condition, torsional stiffness k_t can be described as shown in Fig. 2(a), and is proportional to the bulk shear modulus G_{bulk}, boundary condition constant κ, and the polar moment of inertia I_p, and inversely proportional to the spring length L. Bulk shear modulus in a torsion beam with a rectangular cross-section can be derived from

$$G_{bulk} = \int_0^{\frac{1}{2}} \int_0^{\frac{1}{2}} \frac{48 G_\psi \left(x^2 + r^2 \cdot y^2 \right)}{\left(1 + r^2 \right)} dx \cdot dy , \qquad (1)$$

where G_ψ is the conventional shear modulus, as shown in Fig. 1, x is the normalized x-directional coordinate with respect to the spring width, y is the normalized y-directional coordinate with respect to the spring thickness, and r is the aspect ratio of spring thickness to spring width. Bulk shear modulus in terms of angle ψ can be transformed in terms of normalized coordinates x and y by (2).

$$\tan \psi = \frac{r \cdot y}{x} \qquad (2)$$

From (1), the bulk shear modulus can be derived as (3), (4), and (5) in silicon (100), (110), and (111), respectively. The variable α represent the angle from the <100>-axis to the <010>-axis on the <001> plane. The variable β represents the angle from the <001>-axis to the <-110>-axis on the <110> plane. The variable γ represents the angle from the <1-10>-axis to the <-1-12>-axis on the <111> plane. Compliance coefficient S_{44} has 1.26×10^{-2}/GPa and S_c has 0.352×10^{-2}/GPa.

The bulk shear moduli were evaluated and plotted in Fig. 2. In the case of silicon (001), the bulk shear modulus has symmetry on the <100>-axis, the <010>-axis, and the <110>-axis. Regardless of aspect ratio r, the bulk shear modulus on the <100>-axis and the <010>-axis always has the value 79.4 GPa. As the aspect ratio approaches 0, the shape of the bulk shear modulus plot converges to that of the shear modulus $G_\perp = 79.4$ GPa plot in Fig. 1(e). As the aspect ratio approaches infinity, the shape of the bulk shear modulus plot converges to that of the shear modulus $G_{//}$ plot in Fig. 1(e). The maximum difference of the bulk shear modulus increases from 16.2 GPa to 28.3 GPa, as the aspect ratio is increased from 1 to 10. In the case of silicon (110), the bulk shear modulus has symmetry only on the <001>-axis. Regardless of the aspect ratio r, the bulk shear modulus on the <001>-axis is always 79.4GPa. As

the aspect ratio approaches 0, the shape of the bulk shear modulus plot converges to that of the shear modulus $G_\perp$ plot in Fig. 1(f). As the aspect ratio approaches infinity, the shape of the bulk shear modulus plot converges to that of the shear modulus $G_{//}$ plot in Fig. 1(f). The maximum difference of bulk shear modulus increases from 21.6 GPa to 23.4 GPa, as the aspect ratio is increased from 1 to 10. The variation of bulk shear modulus in the <-110>-axis becomes 15.8 GPa as the variation of the aspect ratio from 1 to 10. In the case of silicon (111), the bulk shear modulus has repeatibility from $\gamma = 30°$, $\gamma = 150°$, and $\gamma = 270°$. As the aspect ratio approaches 0, the shape of the bulk shear modulus plot converges to that of the shear modulus $G_\perp$ plot in Fig. 1(g). As the aspect ratio approaches infinity, the shape of the bulk shear modulus plot converges to that of the shear modulus $G_{//}$ plot in Fig. 1(g). The maximum difference of bulk shear modulus decreased from 19.9 GPa to 4.4 GPa, as the aspect ratio increased from 1 to 10. As tabulated in Table 1, the variations in bulk shear modulus for the three different types of silicon are similar for an aspect ratio of 1. For a higher aspect ratio beam, which is generally used for torsional springs, the variation of (111) silicon is substantially smaller, compared to the other types of silicon examined.
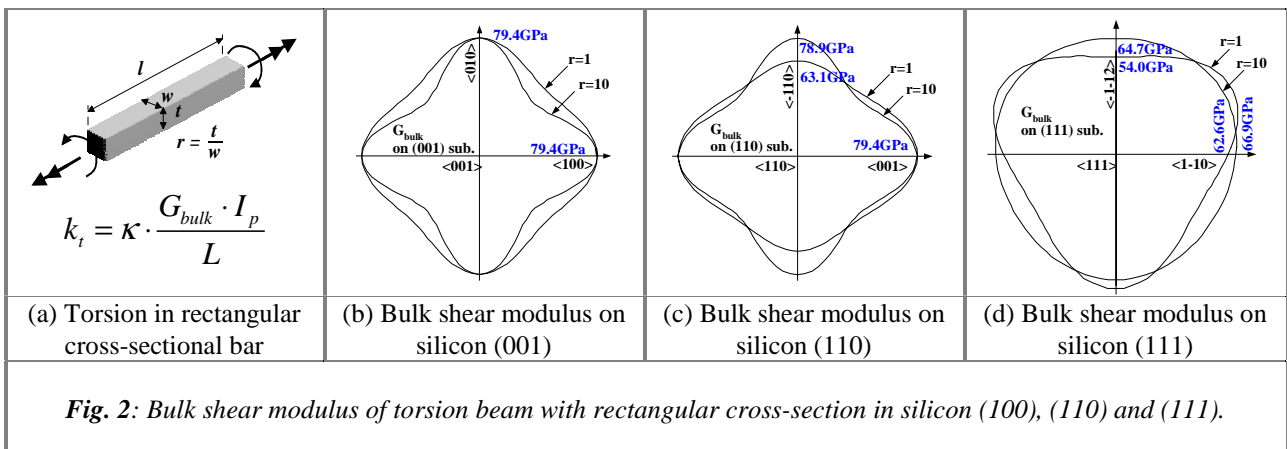
CONCLUSION

Young's modulus, Poisson's ratio, and shear modulus for transverse and vertical motion are independent of device crystallographic orientation, only on silicon (111). Torsional motion is governed by "bulk shear modulus" and device geometry, and the variation of bulk shear modulus with respect to crystallographic orientation is the smallest on silicon (111). Therefore, single-crystal silicon MEMS devices fabricated using (111) silicon will be least sensitive to device orientation with respect to crystallographic orientations. Furthermore, since less restriction is imposed on mask designs with respect to crystallographic orientation, the design task becomes much easier.

$$G_{(100)bulk}(\alpha, r) = \int_0^{0.5}\int_0^{0.5} \frac{48\left(x^2 + r^2 y^2\right)^2 \big/ \left(1 + r^2\right)}{S_{44}\left(x^2 + r^2 y^2\right) + 2S_c \cdot \sin^2 2\alpha \cdot r^2 y^2}\, dx\,dy \tag{3}$$

$$G_{(110)bulk}(\beta, r) = \int_0^{0.5}\int_0^{0.5} \frac{48\left(x^2 + r^2 y^2\right)^2 \big/ \left(1 + r^2\right)}{\left(S_{44} + 2S_c \sin^2 \beta\right)\left(x^2 + r^2 y^2\right) + 2S_c \sin^2 \beta\left[3\cos^2 \beta - 1\right] r^2 y^2}\, dx\,dy \tag{4}$$

$$G_{(111)bulk}(\gamma, r) = \int_0^{0.5}\int_0^{0.5} \frac{144\left(x^2 + r^2 y^2\right)^2 \big/ \left(1 + r^2\right)}{\left(3S_{44} + 4S_c\right) x^2 + \left(3S_{44} + 2S_c\right) r^2 y^2 - 4\sqrt{2} S_c r x y \sin 3\gamma}\, dx\,dy \tag{5}$$

(a) Young's modulus on silicon (100)	(b) Young's modulus on silicon (110)	(c) Poisson's ratio on silicon (100)	(d) Poisson's ratio on silicon (110)
(e) Shear modulus on silicon (100)	(f) Shear modulus on silicon (110)	(g) Young's modulus and Shear modulus on silicon (111)	(h) Poisson's ratio on silicon (111)

Fig. 1: *Young's modulus, Poisson's ratio, and shear modulus on silicon (100), (110) and (111).*

(a) Torsion in rectangular cross-sectional bar	(b) Bulk shear modulus on silicon (001)	(c) Bulk shear modulus on silicon (110)	(d) Bulk shear modulus on silicon (111)

Fig. 2: *Bulk shear modulus of torsion beam with rectangular cross-section in silicon (100), (110) and (111).*

Table 1: *Bulk shear modulus of torsion beam in silicon (100), (110) and (111).*

[GPa]		(100)	(110)	(111)
r = 1	Max	79.4	79.4	73.9
	Min	63.2	57.8	54.0
	Variation	16.2	21.6	19.9
R = 10	Max	79.4	79.4	69.1
	Min	51.2	56.0	64.7
	Variation	28.3	23.4	4.4

REFERENCES

[1] K. A. Shaw, Z. L. Zhang, and N. C. MacDonald, "SCREAM I: A single mask, single-crystal silicon, reactive ion etching process for microelectromechanical structures," *Sensors and Actuators A*, 40, pp. 63-70, 1994.

[2] B. Diem, M. T. Delaye, F. Michel, S. Renard, and G. Delapoerre, "SOI (SIMOX) as a substrate for surface micromachining of single crystalline silicon sensors and actuators," in *Proceeding of the 7th International Conference on Solid-State Sensors and Actuators (Transducers '93)*, Yokohama, Japan, June 1993, pp. 233-236.

[3] S. T. Cho, "A batch dissolved wafer process for low cost sensor applications," in *SPIE Proceeding of Micromachining and Microfabrication Process Technology*, Austin, USA, September 1995, pp. 10-17.

[4] T. E. Bell, P. T. J. Gennissen, D. DeMunter, and M. Kuhl, "Porous silicon as a sacrificial material," *IOP Journal of Micromechcal and Microengineering*, vol. 6, pp. 361-369, 1996.

[5] S. Lee, S. Park, and D. Cho, "A new micromachining technology using (111) silicon," in *Digest of papers on Microprocess and Nanotechnology Conference*, Kyongju, Korea, June 1998, pp. 174-175. (also in *Japanese Journal of Applied Physics*, vol. 38, pp. 2699-2703, May 1999.)

[6] S. Lee, S. Park, S. Yi, S. Lee, D. Cho, B. Ha, Y. Oh, and C. Song, "Electrostatic actuation of surface/bulk micromachined single-crystal silicon microresonators," in *Proceeding of IEEE/RSJ International Conference on Intelligent Robots and Systems*, Kyongju, Korea, October 1999, vol. 2, pp. 1057-1062.

[7] S. Park, S. Lee, S. Yi, and D. Cho, "Mesa-supported, single-crystal microstructures fabricated by the Surface/Bulk Micromachining (SBM) process," *Japanese Journal of Applied Physics*, vol. 38, pp. 4244-4249, July 1999.

[8] S. Lee, S. Park, and D. Cho, "Surface/Bulk Micromachining (SBM) process and deep trench oxide isolation method for MEMS," in *Proceeding of International Electron Devices Meeting*, Washington D. C., USA, December 1999, pp. 701-704.

[9] S. Lee, S. Park, and D. Cho, "The Surface/Bulk Micromachining (SBM) process: a new method for fabricating released microelectromechanical systems in single crystal silicon," *IEEE/ASME Journal of Microelectromechanical Systems*, vol. 8, no. 4, pp. 409-416, December 1999.

[10] D. Cho, S. Lee, and S. Park, "Surface/Bulk micromachined high performance silicon micro-gyroscope," in *Proceeding of 2000 Solid-state Sensor and Actuator Workshop (Hilton Head)*, Late News Paper, Hilton Head Island, SC, USA, June 2000.

[11] S. Lee, S. Park, J. Kim, S. Yi, and D. Cho, "Surface/Bulk micromachined single-crystalline silicon micro-gyroscope," *IEEE/ASME Journal of Microelectromechanical Systems*, vol. 9, no. 4, pp. 557-567, December 2000.

[12] J. J. Wortman and R. A. Evans, "Young's modulus, shear modulus, and Poisson's ratio in silicon and germanium, " *J. Appl. Phys.*, Vol. 36, pp.153-156, 1965.

[13] W. A. Brantley, "Calculated elastic constants for stress problems associated with semiconductor devices, " *J. Appl. Phys.*, Vol. 44, pp.534-535, 1973.

[14] Y. C. Fung, *Foundation of Solid Mechanics*, Prentice-Hall, 1965.

[15] L. E. Malvern, *Introduction to the Mechanics of a Continuous Media*, Prentice-Hall, 1969.

[16] R. A. Conant, J. T. Nee, K. Y. Lau, and R. S. Muller, "A flat high-frequency scanning micromirror," in *Proceeding of 2000 Solid-state Sensor and Actuator Workshop (Hilton Head)*, Hilton Head Island, SC, USA, June 2000, pp.6-13.